



# HHS Public Access

Author manuscript

*ACS Chem Neurosci.* Author manuscript; available in PMC 2022 July 11.

Published in final edited form as:

*ACS Chem Neurosci.* 2019 September 18; 10(9): 4145–4150. doi:10.1021/acchemneuro.9b00347.

## Surface-Modified G4 PAMAM Dendrimers Cross the Blood–Brain Barrier Following Multiple Tail-Vein Injections in C57BL/6J Mice

Bhairavi Srinageshwar<sup>†,‡,§</sup>, Anthony Dils<sup>†,§</sup>, John Sturgis<sup>†,§</sup>, Anna Wedster<sup>§</sup>, Balachandar Kathirvelu<sup>‡,§</sup>, Stephanie Baiyasi<sup>‡</sup>, Douglas Swanson<sup>||</sup>, Ajit Sharma<sup>||</sup>, Gary L. Dunbar<sup>‡,§,⊥,♯</sup>, Julien Rossignol<sup>\*,†,‡,§</sup>

<sup>†</sup>College of Medicine, Central Michigan University, Mt. Pleasant 48859, Michigan, United States

<sup>‡</sup>Field Neurosciences Institute Laboratory for Restorative Neurology, Central Michigan University, Mt. Pleasant 48859, Michigan, United States

<sup>§</sup>Program in Neuroscience, Central Michigan University, Mt. Pleasant 48859, Michigan, United States

<sup>||</sup>Department of Chemistry & Biochemistry, Central Michigan University, Mt. Pleasant 48859, Michigan, United States

<sup>⊥</sup>Department of Psychology, Central Michigan University, Mt. Pleasant 48859, Michigan, United States

<sup>♯</sup>Field Neurosciences Institute, St. Mary's of Michigan, Saginaw 48604, Michigan, United States

### Abstract

Intracranial injections are currently used to deliver drugs into the brain, as most drugs cannot cross the blood–brain barrier (BBB) following systemic injections. Moreover, multiple dosing is difficult with invasive techniques. Therefore, viable systemic techniques are necessary to facilitate treatment paradigms that require multiple dosing of therapeutics across the BBB. In this study, we show that mixed-surface fourth-generation poly(amidoamine) (PAMAM) dendrimers containing predominantly biocompatible hydroxyl groups and a few amine groups are taken up by cultured primary cortical neurons derived from mouse embryo. We also show that these dendrimers cross the BBB following their administration to healthy mice in multiple doses via tail-vein injections and are taken up by neurons and the glial cells as evidenced by appropriate staining methods. Besides the brain, the dendrimers were found mostly in the kidneys compared to other peripheral organs, such as liver, lungs, and spleen, implying that they may be readily excreted, thereby preventing potential toxic accumulation in the body. Our findings provide a proof-of-concept that appropriate surface modifications of dendrimers provide safe, biocompatible nanomaterial with

\*Corresponding Author rossij@cmich.edu. Phone: +1-989-774-3405.

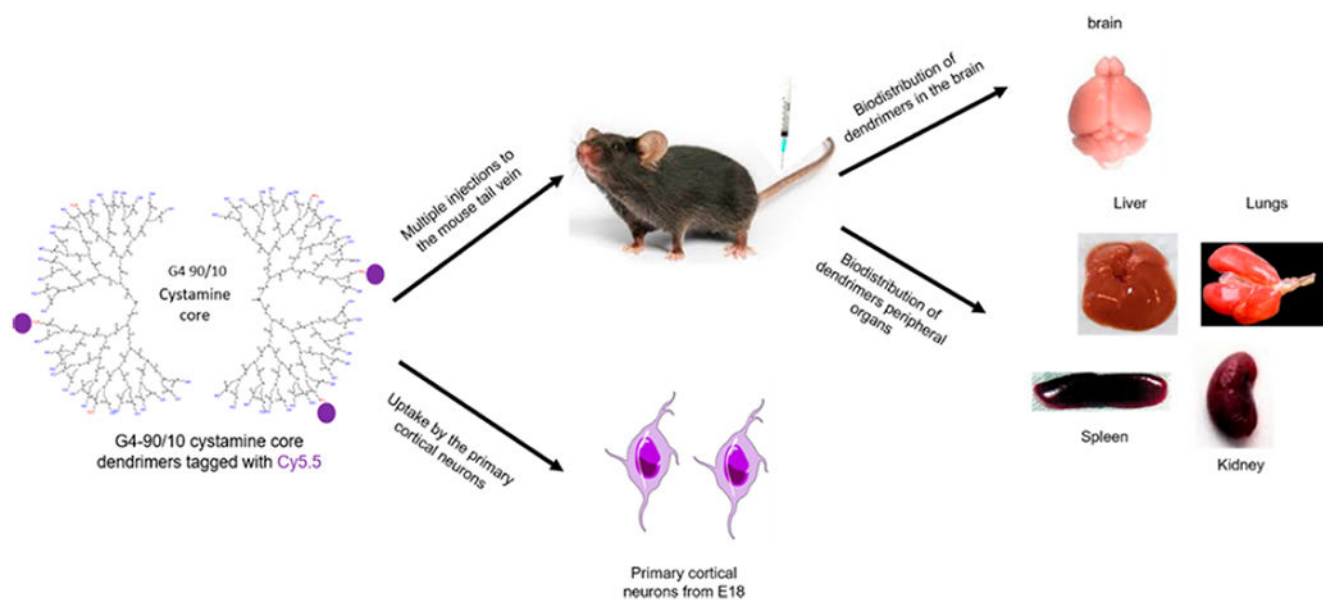
Author Contributions

B.S. conducted the experiments of the study, participated in the design of the study, and helped draft the manuscript. A.D. and J.S. conducted the experiments of the study and participated in the design of the study. A.W. helped with tissue processing. B.K. helped with tail-vein injections, proofreading, and manuscript editing. S.B. helped with mouse handling and maintaining the animal colony. D.S. synthesized the dendrimers used in this study. G.L.D., A.S., and J.R. conceived the study, participated in the design and coordination, edited, and performed the final proof of the manuscript.

The authors declare no competing financial interest.

the potential to deliver therapeutic cargo across the BBB into the brain via multiple tail-vein injections.

## Graphical Abstract



## Keywords

PAMAM dendrimer; blood-brain barrier; multiple injections; tail-vein injections; systemic injections; dendrimer surface

## INTRODUCTION

Poly(amidoamine) (PAMAM) dendrimers are three-dimensional nanomolecules that have various applications in the field of biology and medicine. Extensive reviews on dendrimers and their structure, properties, and biomedical applications (such as drug and nucleic acid delivery) have been previously published.<sup>1-6</sup> In brief, PAMAM dendrimers have three major components: (1) core; (2) branched region that varies with generation (G; such as G1 is ~1 nm in diameter; G2 is ~2 nm in diameter, and so forth); and (3) surface, which typically has one type of functional group (amine, hydroxyl, or carboxyl). The functional groups present on the surface of the dendrimer determine the toxicity of this nanomolecule. For example, many studies have highlighted the toxicity of the 100% amine surface ( $-\text{NH}_2$ ) dendrimers due to their very high positive charge density that causes formation of nanoscale holes in the cell membrane, leading to cell death, while dendrimers with surface carboxyl or hydroxyl groups show much better safety profiles.<sup>7-11</sup> Moreover, an *in vivo* study using a higher-generation cationic dendrimers showed an intravascular coagulation-like condition in mice.<sup>12</sup> An *in vitro* study using platelets showed that PAMAM G7 cationic dendrimers alter platelet morphology and activate them, leading to disrupted platelet function.<sup>13</sup> However, lower-generation PAMAM dendrimers, such as G0–G3, were found to be safe *in vitro*<sup>14</sup> and in biological systems following nasal absorption.<sup>15,16</sup>

Although hydroxyls or carboxyls provide a biocompatible surface, amines are necessary to allow cellular uptake of the dendrimers and for labeling them with fluorescent dyes (or other imaging agents with commercially available bioconjugation reagents designed for proteins) or for electrostatic binding and subsequent transport of nucleic acid cargo. The detailed mechanism of how dendrimers enter cells, especially neurons, is not known. Some of the general hypotheses for dendrimer uptake by the cells include: (1) clathrin-mediated endocytosis, (2) caveolae-mediated endocytosis (specifically for G4 dendrimers), and (3) macropinocytosis.<sup>17</sup>

Using traditional PAMAM dendrimer synthesis protocols (with high reagent excess), we successfully synthesized, de novo, dendrimers with desired amounts of amines and hydroxyls (e.g., 10% amines and 90% hydroxyls or 30% amines and 70% hydroxyls). These mixed-surface dendrimers, like traditional dendrimers, are precise as seen on polyacrylamide gel electrophoresis (PAGE) gels. In addition, they not only offer a more biocompatible surface but also allow binding of nucleic acids and are readily labeled by fluorescent dyes.<sup>18</sup> A representation of a G4 PAMAM dendrimer with 10% amines and the remaining 90% neutral hydroxyl (–OH) groups, known as G4-90/10 (which we shall abbreviate as D) is shown in Figure 1. Although the safety of these dendrimers has not been rigorously assessed, we have observed an eightfold decrease in cell death compared to the pure amine surface dendrimers, on a variety of cells lines (unpublished data). Toxicity of any macromolecule with abundant cationic amines, including PAMAM dendrimers with 100% surface amines, is well-documented in literature,<sup>7-11</sup> which is why we replaced 90% of the amines with nontoxic, biocompatible –OH groups.

Details on the G4-90/10 mixed-surface dendrimer synthesis and characterization, labeling with fluorescent dyes, and their uptake by mouse-derived primary cortical culture can be found in our previous publication.<sup>18</sup> We have also shown that these dendrimers have sufficient positive charge density on their surface to be able to cross the blood-brain barrier (BBB) when injected via the carotid artery in a healthy mouse with an intact BBB.<sup>18</sup> The BBB consists of a monolayer of cells, such as pericytes, astrocytes, and immune cells, which form a certain barrier between the central nervous system (CNS) and the circulatory system.<sup>19-21</sup> The tight junctions form 1 to 4 nm pore size, which enable only selected molecules to pass through them.<sup>22</sup> The two major membrane proteins associated with the tight junction are occludins and claudins.<sup>23</sup> Breakdown of these proteins leads to a disrupted and leaky BBB.<sup>24</sup> The major functions of the BBB are to provide a tight barrier to avoid unwanted exchange of molecules, proteins, enzymes, and solutes from entering the CNS. The BBB also provides an optimal environment for proper signaling functioning of the neurons.<sup>25</sup> Since the BBB is not permeable to large molecules, it is a major barrier to deliver drugs to the CNS following systemic injections.<sup>26</sup> The advantage of injecting a drug-loaded dendrimer into the carotid artery is that the drugs may reach the brain at high concentrations without significant uptake by peripheral organs.<sup>27</sup> Though the dendrimers were not found in the kidneys, it was not known whether the dendrimers injected via the carotid were being eliminated from the biological system, since the mere absence of dendrimers in the kidneys does not confirm excretion.<sup>18</sup> Although current endovascular techniques allow targeted delivery to the brain by carotid injections, there are disadvantages associated with this route, such as the need for highly skilled professionals and a possibility of drug loss over

extended time periods.<sup>28</sup> Considering the potential pitfalls of injecting drugs via the carotid artery, there is a critical need for an alternate route of delivering dendrimers or dendrimer-carrying drugs to the brain. In this study, we injected cyanine 5.5 (Cy5.5)-labeled G4-90/10 dendrimers (D-Cy5.5) multiple times with increasing concentrations at four different time points via the tail-vein of healthy mice with intact BBB to determine if these dendrimers are able to cross the BBB following venous administration.

## RESULTS

### Dendrimer Labeling.

The dendrimers were successfully labeled with Cy5.5, which was confirmed using acidic native PAGE as described previously.<sup>18,29</sup>

### D-Cy5.5 Uptake by Mouse-Derived Primary Cortical Culture.

The D-Cy5.5 was readily taken up by the primary cortical culture (PCC) at the specified concentration when incubated for 30 min. Colocalization between the Hoechst stain and Cy5.5 was observed, indicating that the dendrimers were able to cross the cell membrane and enter the cells (Figure 2).

### Uptake of D-Cy5.5 Dendrimers by the Brain Following Administration via Tail-Vein.

D-Cy5.5 was administered to the mice via tail-vein injections at four different concentrations and at different time-points as mentioned in the Methods section. The animals were sacrificed 24 h following the last injection. The D-Cy5.5 dendrimers were able to cross the BBB, and the biodistribution of the dendrimers in the brain is shown in Figure 3.

At a higher magnification, colocalization between the Hoechst and the D-Cy5.5 was observed, confirming that the D-Cy5.5 was taken up by the cells of the brain (Figure 4).

### Uptake of the D-Cy5.5 by Peripheral Organs.

Peripheral sections showed that the D-Cy5.5 was taken up by the kidneys, liver, lungs, and spleen (Figure 5). Among the different peripheral organs analyzed, kidney cells and the renal calyx had the maximum accumulated dendrimers compared to liver, lungs, and spleen.

These results contrast with our previous study, where we injected the same dendrimers, tagged with fluorescein isothiocyanate (FITC) via the carotid artery, and did not find any significant dendrimer accumulation in the peripheral organs.

### Uptake of D-Cy5.5 by Neurons and Glial Cells.

Colocalization between Hoechst and D-Cy5.5 with neuronal nuclei (NeuN; Figure 6) and glial fibrillary acidic protein (GFAP; Figure 7) showed that the D-Cy5.5 crossed the BBB when injected via the tail-vein and were taken up by the neurons and glial cells, respectively.

## DISCUSSION

PAMAM dendrimers that are commercially available typically contain a pure surface such as amine, carboxyl, or hydroxyl. The cationic amine surface is the most popular, since it can easily be modified, provide attachment sites for anionic nucleic acids, fluorescent dyes, and other imaging agents or drugs.<sup>9</sup> Attaching a precise amount of a ligand to the surface of a typical dendrimer such as a G4 or G5, which have 64 and 128 amine groups on their surface, respectively, is extremely challenging.<sup>30</sup>

We prepared mixed-surface dendrimers de novo, similar to the synthesis of traditional pure surface dendrimers, using high reagent excess as previously described. When subjected to analysis by separation techniques such as electrophoresis and high-performance liquid chromatography (HPLC), these mixed-surface dendrimers were found to be as structurally precise as the traditional dendrimers. The presence of amines alone is not the reason for toxicity of nanomaterials; otherwise, most proteins would be toxic to cells. Instead, the number of amines per given surface area better correlates with biocompatibility. A 10% amine/90% hydroxyl surface G4 dendrimer was found to be less toxic than pure amine surface dendrimers on cell viability (unpublished data). Safety and product reproducibility of nanomaterials are two essential criteria for potential use in the clinic.<sup>2</sup> In addition, this dendrimer had sufficient cationic surface characteristics to enter cells, probably by adsorptive endocytosis. Carotid injection also allowed the dendrimer to cross the BBB and gain entry to the brain. The present results show that this mixed-surface dendrimer can also enter the brain via a systemic tail-vein injections, which constitutes a more practical and clinically relevant route of administration. Once in the brain, the dendrimers enter both neurons and glial cells. Our previous study showed that these modified-surface dendrimers, tagged with FITC, were taken up by PCC as well as by the neurons and glial cells, in vivo, following carotid injections.<sup>18</sup>

Lesniak and colleagues<sup>31</sup> modified the surface of pure hydroxyl surface G4 ethylenediamine (EDA) core PAMAM dendrimer to produce a material with ~6% amines (four amines per G4 molecule). This was done by reacting commercial G4 pure hydroxyl surface dendrimer with 6-(Fmoc-amino) caproic acid, followed by piperidine/dimethylformamide treatment to generate the free amines. The fluorescent dye Cy5 was then conjugated to the amine-modified dendrimer, with an average of one dye per dendrimer. The dendrimer was then injected by tail-vein into neonatal rabbits as a single dose of 800  $\mu\text{g}$  per animal. The dendrimer used by Lesniak and colleagues was quite similar to the one we used in our study, except for a slightly greater number of amines (six amines per dendrimer, as determined by the trinitrobenzenesulfonic acid (TNBSA) assay for amines) in our Methods section of synthesis. In addition, we studied mice, instead of neonatal rabbits, and used a total dose of 390  $\mu\text{g}$  dendrimer per mouse. However, instead of a bolus dose used by Lesniak and colleagues, our dosing schedule was 40, 50, 100, and 200  $\mu\text{g}$  (all in 100  $\mu\text{L}$  volume), every other day. Assuming that mice and neonatal rabbits have comparable weights (~25 to 30 g), our total dose on a weight basis is approximately half that of the study conducted by Lesniak and colleagues. Their study showed that the dendrimers were mainly found in the kidneys (especially in the convoluted tubular cells), similar to our findings. In addition, their study also found smaller amounts of dendrimers in the liver, lungs, and heart, while we found

smaller amounts in the liver, lungs, and spleen. The ability to find our dendrimers in the brain of healthy animals may be due to the dosage regimen. We found the dendrimers in the brain following single dose (40  $\mu\text{g}/\text{animal}$ ) injection into the carotid artery.

In another related study, Sadekar and colleagues<sup>32</sup> performed a comprehensive study on the biodistribution of radiolabeled pure hydroxyl surface PAMAM G5–G7 dendrimers in mice with orthotopically inoculated ovarian tumor, after injection of a single dose of ~1500  $\mu\text{g}$  dendrimers per animal, assuming mouse weight of 30 g. They found the G5 PAMAM dendrimers (which are twice as large as G4 dendrimer) accumulated mainly in the kidneys, one-tenth to one-fifteenth the amount of accumulation in the liver and spleen. G6 (fourfold larger than G4) accumulated in equal amounts both in the kidneys and liver, while G7 (approximately eightfold larger than G4) showed an extended plasma half-life and accumulated in the heart, lungs, liver, spleen, and kidneys in equal amounts. Interestingly, a small amount of G7 (but not G5 or G6) was also seen in the brain.<sup>32</sup>

As mentioned earlier, G4 dendrimers are ~4 nm in diameter, and it has been shown that the filtration size cutoff for the kidneys is 3.7–6 nm.<sup>33</sup> Our findings indicate that most of the injected mixed-surface dendrimers were detected in the kidneys, compared to other organs, which is consistent with those of studies conducted by Lesniak and Sadekar groups. This may be an indication that the dendrimers could be in the process of renal excretion; however, more confirmation assays are necessary to prove. If this is the case, then the ability of the kidneys to excrete the dendrimers avoids potential accumulation within the body and potential long-term toxic effects of the vehicle. This is an important criterion to consider when using dendrimers as vehicles to carry cargo.

Collectively, our work, together with that of Lesniak and colleagues, suggests that the G4 mixed-surface dendrimer, consisting of a predominantly hydroxyl coating and a few amines, has the potential of delivering drugs to the brain when dosed appropriately. The low levels of the nanomolecule detected in other organs compared to the kidneys are promising features indicating that the distribution of the dendrimers reduces risk of potential accumulation of the xenobiotic in the body.

## METHODS

### PAMAM Dendrimer Synthesis.

The surface-modified G4-90/10 dendrimer having a diaminobutane (DAB) core was synthesized and fluorescently tagged with cyanine 5.5 (Lumiprobe; D-Cy5.5) as described previously.<sup>18</sup> The labeled dendrimers were dialyzed overnight using 0.9% sodium chloride followed by dialysis in water. The dialyzed Cy5.5-labeled dendrimers were lyophilized for 48 h and stored at  $-20\text{ }^{\circ}\text{C}$  until further use.

### In Vitro Uptake of D-Cy5.5 by the Mouse-Derived Primary Cortical Culture (PCC).

The primary cortical culture from mouse at embryonic stage 18 (E18) (Aug 16, 2018, and was registered under the Central Michigan University (CMU) Institutional Animal Care and Use of Committee (IACUC) protocol #18–23) as extracted and cultured for 14 days as described in our previous publication.<sup>18</sup> The cells were incubated with D-Cy5.5 at a final

concentration of 4 mg/mL for 30 min. The cell nucleus was labeled with Hoechst 33342 (Thermo Fisher Scientific) and fixed using 4% paraformaldehyde (PFA; Sigma-Aldrich). The cells were grown on coverslips and were imaged using a Zeiss Observer inverted microscope (Zeiss).

## In Vivo.

**Animals and Groups.**—Nine in-house bred C57BL/6J male and female mice aged between 5 and 15 weeks old were used in this study. All mice were group-housed in clear polycarbonate containers with sawdust bedding and ad libitum access to food and water. The room temperature was set at 22 °C and on a 12 h light/dark cycle (lights ON at 12 AM). All the experimental procedures followed the guidelines of the IACUC of CMU (Aug 16, 2018, and was registered under the CMU IACUC protocol #18–23). The animals were randomly divided into two major groups: D-Cy5.5 group ( $n = 6$ ) and Hank's balanced salt solution (HBSS) group ( $n = 3$ ).

**Dendrimer Dosing and Frequency.**—All animals received 100  $\mu\text{L}$  of either HBSS or D-Cy5.5 via tail-vein on days 1, 3, 5, and 7. The animals that received D-Cy5.5 were given an increasing concentration starting at 40  $\mu\text{g}$  on day 1 and at 50, 100, and 200  $\mu\text{g}$  on days 3, 5, and 7, respectively.

**D-Cy5.5 Administration into the Tail-Vein.**—All animals were anesthetized with a gaseous mixture of isoflurane and oxygen and secured in a mouse restrainer (Braintree Scientific, Inc.) at the edge of the table. The tail was gently cleaned with chlorhexidine (Molnlycke Healthcare), dipped in a 15 mL centrifuge tube filled with warm water to facilitate exposure of the veins, and later wiped with a sterile gauze before injection. A 25 G needle was inserted at an angle almost parallel to the vein, advanced  $\sim 5$  mm, and withdrawn slightly to verify correct placement, via back pressure and blood entering the housing of the needle. The plunger was depressed slowly pushing the entire 100  $\mu\text{L}$  of HBSS/D-Cy5.5. After the needle gently was removed, the tail was compressed with alcohol wipes and later moved to a heated recovery box until ambulatory.

**Euthanasia and Tissue Preparation.**—Twenty-four hours following the last injection, the animals were sacrificed by cervical dislocation. Different organs such as brain, liver, lungs, spleen, and kidneys were extracted and fixed using 4% PFA (Sigma-Aldrich) for 48 h. Following this procedure, the various organs were transferred to 30% sucrose until they sank and were then frozen using 2-methylbutane (Sigma-Aldrich). The frozen tissue was stored at  $-80$  °C until further processing.

## Histology.

All the frozen tissue was sliced in sagittal plane beginning from medial to lateral ends at 30  $\mu\text{m}$  using cryostat. The brain tissue was stained using Hoechst 33342 (Thermo Fisher Scientific) at a concentration of 0.01 mg/mL. To analyze the uptake of the D-Cy5.5 by the neurons and glial cells, the tissue was stained using anti-rabbit-neuronal nuclei antibody (NeuN 1/3000; ab177487, Abcam), diluted in phosphate-buffered saline with 0.1% triton X-100 (Fluka chemicals) and anti-rabbit-glial fibrillary acidic protein antibody (GFAP;

1/2000; ab7260 Abcam), diluted in phosphate-buffered saline with 0.3% triton X-100 (Fluka chemicals). The stained tissue sections were mounted on positively charged glass slides, coverslipped, and viewed using Zeiss Axio Imager M1 microscope (Carl Zeiss AG).

## CONCLUSION

This study proves that the mixed-surface dendrimers can cross the BBB following multiple via tail-vein injections. In addition to the dendrimers reaching the brain, they were also found in the kidneys of the healthy adult mice, which may be an indication of the dendrimers getting eliminated from the biological systems and can function as safe cargo carriers for delivering potential therapeutics, such as drugs, genes, and gene-editing tools.

## FUTURE DIRECTIONS

This study has confirmed the uptake of the dendrimers by the neurons and glia in the brain following tail-vein injections. The percentage of the number of neurons versus the glia uptake and the fate of the dendrimers/renal elimination from the biological system following systemic injections are a part of our future directions.

## Funding

Support for this study was provided by the Program in Neuroscience, the College of Medicine, the Chemistry & Biochemistry Department, and the John G. Kulhavi Professorship in Neuroscience at Central Michigan University and the Field Neurosciences Institute.

## ABBREVIATIONS

<b>BBB</b>	blood-brain barrier
<b>FITC</b>	fluorescein isothiocyanate
<b>Cy5.5</b>	Cyanine 5.5
<b>EDA</b>	ethylenediamine
<b>NeuN</b>	Neuronal nuclei
<b>GFAP</b>	Glial fibrillary acidic protein
<b>PAMAM</b>	poly(amidoamine)
<b>DAB</b>	diaminobutane
<b>HPLC</b>	high performance liquid chromatography
<b>HBSS</b>	Hank's balanced salt solution
<b>PCC</b>	primary cortical culture
<b>PFA</b>	paraformaldehyde



## REFERENCES

- (1). Kannan RM, Nance E, Kannan S, and Tomalia DA (2014) Emerging Concepts in Dendrimer-Based Nanomedicine: From Design Principles to Clinical Applications. *J. Intern. Med* 276 (6), 579–617. [PubMed: 24995512]
- (2). Florendo M, Figacz A, Srinageshwar B, Sharma A, Swanson D, Dunbar GL, and Rossignol J (2018) Use of Polyamidoamine Dendrimers in Brain Diseases. *Molecules* 23 (9), 2238.
- (3). Otto DP, and de Villiers MM (2018) Poly(Amidoamine) Dendrimers as a Pharmaceutical Excipient. Are We There Yet? *J. Pharm. Sci* 107 (1), 75–83. [PubMed: 29045886]
- (4). Palmerston Mendes L, Pan J, and Torchilin VP (2017) Dendrimers as Nanocarriers for Nucleic Acid and Drug Delivery in Cancer Therapy. *Molecules* 22 (9), 1401.
- (5). Menjoge AR, Kannan RM, and Tomalia DA (2010) Dendrimer-Based Drug and Imaging Conjugates: Design Considerations for Nanomedical Applications. *Drug Discovery Today* 15 (5–6), 171–185. [PubMed: 20116448]
- (6). Esfand R, and Tomalia DA (2001) Poly(Amidoamine) (PAMAM) Dendrimers: From Biomimicry to Drug Delivery and Biomedical Applications. *Drug Discovery Today* 6 (8), 427–436. [PubMed: 11301287]
- (7). Thomas TP, Majoros I, Kotlyar A, Mullen D, Banaszak Holl MM, and Baker JR (2009) Cationic Poly(Amidoamine) Dendrimer Induces Lysosomal Apoptotic Pathway at Therapeutically Relevant Concentrations. *Biomacromolecules* 10 (12), 3207–3214. [PubMed: 19924846]
- (8). De Stefano D, Carnuccio R, and Maiuri MC (2012) Nanomaterials Toxicity and Cell Death Modalities. *J. Drug Delivery* 2012, 167896.
- (9). Márquez-Miranda V, Peñaloza JP, Araya-Durán I, Reyes R, Vidaurre S, Romero V, Fuentes J, Céric F, Velásquez L, González-Nilo FD, et al. (2016) Effect of Terminal Groups of Dendrimers in the Complexation with Antisense Oligonucleotides and Cell Uptake. *Nanoscale Res. Lett* 11 (1), 66. [PubMed: 26847692]
- (10). Zeng Y, Kurokawa Y, Win-Shwe T-T, Zeng Q, Hirano S, Zhang Z, and Sone H (2016) Effects of PAMAM Dendrimers with Various Surface Functional Groups and Multiple Generations on Cytotoxicity and Neuronal Differentiation Using Human Neural Progenitor Cells. *J. Toxicol. Sci* 41 (3), 351–370. [PubMed: 27193728]
- (11). Zhang J, Liu D, Zhang M, Sun Y, Zhang X, Guan G, Zhao X, Qiao M, Chen D, and Hu H (2016) The Cellular Uptake Mechanism, Intracellular Transportation, and Exocytosis of Polyamidoamine Dendrimers in Multidrug-Resistant Breast Cancer Cells. *Int. J. Nanomed* 11, 3677–3690.
- (12). Greish K, Thiagarajan G, Herd H, Price R, Bauer H, Hubbard D, Burckle A, Sadekar S, Yu T, Anwar A, et al. (2012) Size and Surface Charge Significantly Influence the Toxicity of Silica and Dendritic Nanoparticles. *Nanotoxicology* 6 (7), 713–723.
- (13). Jones CF, Campbell RA, Franks Z, Gibson CC, Thiagarajan G, Vieira-de-Abreu A, Sukavaneshvar S, Mohammad SF, Li DY, Ghandehari H, et al. (2012) Cationic PAMAM Dendrimers Disrupt Key Platelet Functions. *Mol. Pharmaceutics* 9 (6), 1599–1611.
- (14). Teow HM, Zhou Z, Najlah M, Yusof SR, Abbott NJ, and D'Emanuele A (2013) Delivery of Paclitaxel across Cellular Barriers Using a Dendrimer-Based Nanocarrier. *Int. J. Pharm* 441 (1–2), 701–711. [PubMed: 23089576]
- (15). Dong Z, Katsumi H, Sakane T, and Yamamoto A (2010) Effects of Polyamidoamine (PAMAM) Dendrimers on the Nasal Absorption of Poorly Absorbable Drugs in Rats. *Int. J. Pharm* 393 (1–2), 245–252.
- (16). Dong Z, Hamid KA, Gao Y, Lin Y, Katsumi H, Sakane T, and Yamamoto A (2011) Polyamidoamine Dendrimers Can Improve the Pulmonary Absorption of Insulin and Calcitonin in Rats. *J. Pharm. Sci* 100 (5), 1866–1878. [PubMed: 21374620]
- (17). Vidal F, Vásquez P, Díaz C, Nova D, Alderete J, and Guzmán L (2016) Mechanism of PAMAM Dendrimers Internalization in Hippocampal Neurons. *Mol. Pharmaceutics* 13 (10), 3395–3403.
- (18). Srinageshwar B, Peruzzaro S, Andrews M, Johnson K, Hietpas A, Clark B, McGuire C, Petersen E, Kippe J, and Stewart A (2017) PAMAM Dendrimers Cross the Blood–Brain Barrier When Administered through the Carotid Artery in C57BL/6J Mice. *Int. J. Mol. Sci* 18 (3), 628.

- (19). Sharif Y, Jumah F, Coplan L, Krosser A, Sharif K, and Tubbs RS (2018) Blood Brain Barrier: A Review of Its Anatomy and Physiology in Health and Disease. *Clin. Anat. N. Y.* N 31 (6), 812–823.
- (20). Keaney J, and Campbell M (2015) The Dynamic Blood-Brain Barrier. *FEBS J.* 282 (21), 4067–4079. [PubMed: 26277326]
- (21). Banks WA (2009) Characteristics of Compounds That Cross the Blood-Brain Barrier. *BMC Neurol.* 9 (Suppl1), S3. [PubMed: 19534732]
- (22). Daneman R, and Prat A (2015) The Blood–Brain Barrier. *Cold Spring Harb. Perspect. Biol* 7 (1), a020412. [PubMed: 25561720]
- (23). Luissint A-C, Artus C, Glacial F, Ganeshamoorthy K, and Couraud P-O (2012) Tight Junctions at the Blood Brain Barrier: Physiological Architecture and Disease-Associated Dysregulation. *Fluids Barriers CNS* 9, 23. [PubMed: 23140302]
- (24). Chen F, Ohashi N, Li W, Eckman C, and Nguyen JH (2009) Disruptions of Occludin and Claudin-5 in Brain Endothelial Cells in Vitro and in Brains of Mice with Acute Liver Failure. *Hepatology* 50 (6), 1914–1923. [PubMed: 19821483]
- (25). Abbott NJ (2013) Blood-Brain Barrier Structure and Function and the Challenges for CNS Drug Delivery. *J. Inherited Metab. Dis* 36 (3), 437–449. [PubMed: 23609350]
- (26). Dong X (2018) Current Strategies for Brain Drug Delivery. *Theranostics* 8 (6), 1481–1493. [PubMed: 29556336]
- (27). Alam MI, Beg S, Samad A, Baboota S, Kohli K, Ali J, Ahuja A, and Akbar M (2010) Strategy for Effective Brain Drug Delivery. *Eur. J. Pharm. Sci* 40 (5), 385–403. [PubMed: 20497904]
- (28). Joshi S, Meyers PM, and Ornstein E (2008) Intracarotid Delivery of Drugs: The Potential and the Pitfalls. *Anesthesiology* 109 (3), 543–564. [PubMed: 18719453]
- (29). Sharma A, Desai A, Ali R, and Tomalia D (2005) Polyacrylamide Gel Electrophoresis Separation and Detection of Polyamidoamine Dendrimers Possessing Various Cores and Terminal Groups. *J. Chromatogr. A* 1081 (2), 238–244. [PubMed: 16038215]
- (30). Mullen DG, Desai AM, Waddell JN, Cheng X-M, Kelly CV, McNerny DQ, Majoros IJ, Baker JR, Sander LM, Orr BG, et al. (2008) The Implications of Stochastic Synthesis for the Conjugation of Functional Groups to Nanoparticles. *Bioconjugate Chem.* 19 (9), 1748–1752.
- (31). Lesniak WG, Mishra MK, Jyoti A, Balakrishnan B, Zhang F, Nance E, Romero R, Kannan S, and Kannan RM (2013) Biodistribution of Fluorescently Labeled PAMAM Dendrimers in Neonatal Rabbits: Effect of Neuroinflammation. *Mol. Pharmaceutics* 10 (12), 4560–4571.
- (32). Sadekar S, Ray A, Janàt-Amsbury M, Peterson CM, and Ghandehari H (2011) Comparative Biodistribution of PAMAM Dendrimers and HPMA Copolymers in Ovarian-Tumor-Bearing Mice. *Biomacromolecules* 12 (1), 88–96. [PubMed: 21128624]
- (33). Rippe C, Asgeirsson D, Venturoli D, Rippe A, and Rippe B (2006) Effects of Glomerular Filtration Rate on Ficoll Sieving Coefficients (Theta) in Rats. *Kidney Int.* 69 (8), 1326–1332. [PubMed: 16395274]

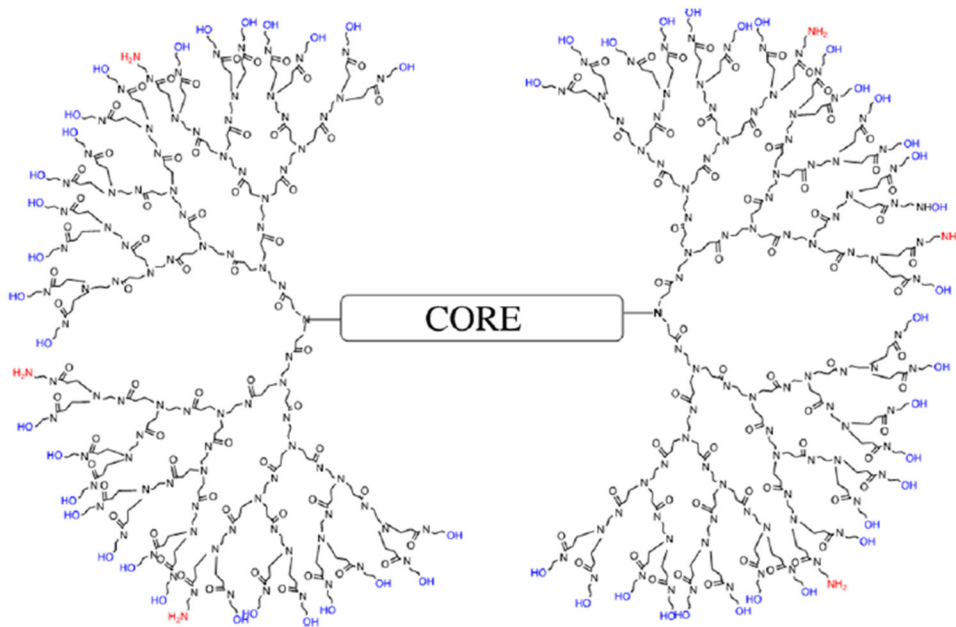


**Figure 1.** Representation of the G4-90/10 dendrimers (D) having 90% hydroxyl groups and 10% amine groups.

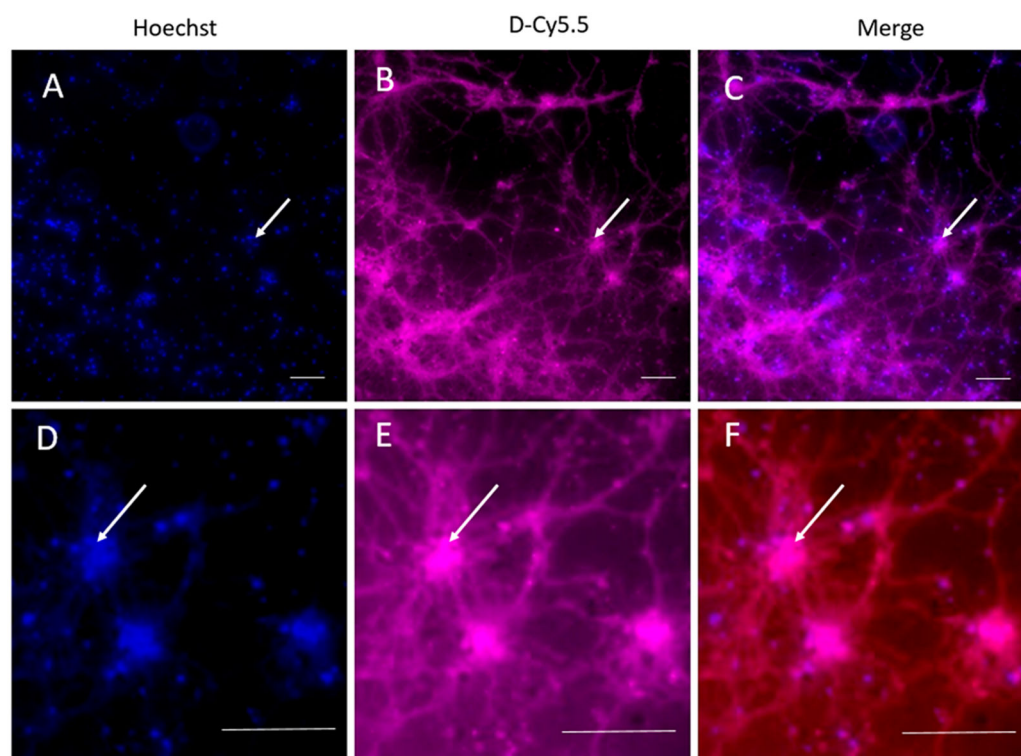


**Figure 2.** Uptake and retention of D-Cy5.5 dendrimers by mouse-derived PCC. Images (D), (E), and (F) are the enlarged images of (A), (B), and (C), respectively. (A) and (D) show the cell nuclei labeled with Hoechst 33342 (arrow). (B) and (E) show uptake of D-Cy5.5 dendrimers by the PCC (arrow). (C) and (F) are merged images of the Hoechst and D-Cy5.5 staining, showing that D-Cy5.5 has reached the nuclei of the neurons (arrow) in addition to entry into their dendrites and axonal branches. Scale bar = 100  $\mu\text{m}$ .

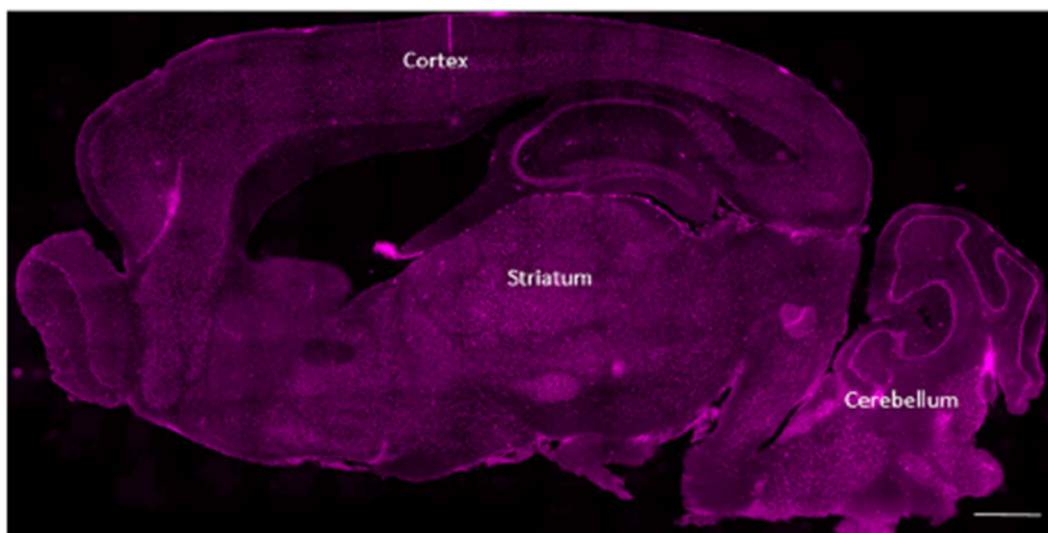


**Figure 3.** Overall biodistribution of the D-Cy5.5 in the brain following tail-vein injections administered at four different concentrations at four different time points. The major anatomical regions such as the cerebral cortex, striatum, and the cerebellum have taken up the D-Cy5.5 in addition to other regions of the brain. Scale bar = 1000  $\mu\text{m}$ .

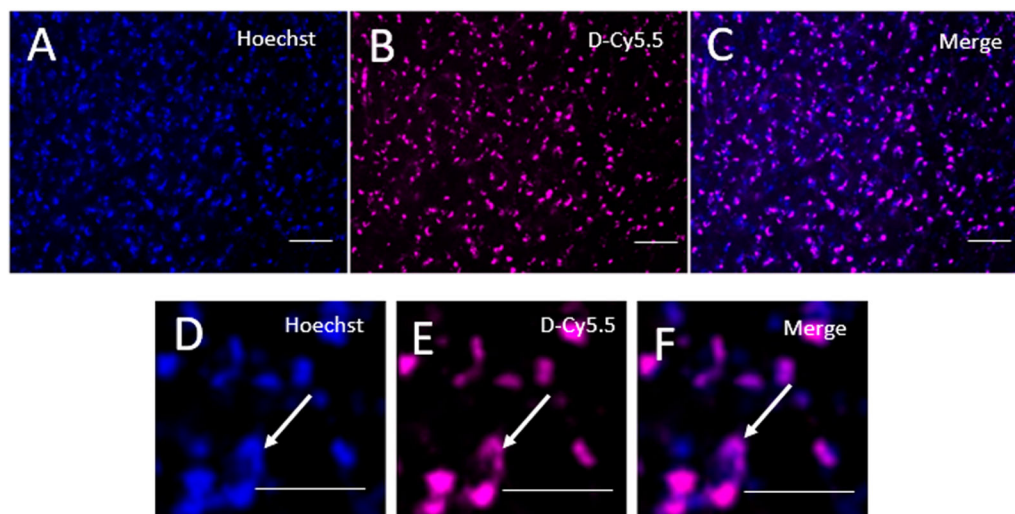


**Figure 4.** Uptake of D-Cy5.5 by the cells in the brain. Images (D), (E), and (F) are the enlarged images of (A), (B), and (C), respectively. (A) and (D) show the cell nuclei labeled with Hoechst 33342 (arrow). (B) and (E) show uptake of the D-Cy5.5 dendrimers by the PCC (arrow) and are merged images between the Hoechst and D-Cy5.5 staining, showing that D-Cy5.5 has reached the nuclei of the neurons (arrow). Scale bar = 20  $\mu\text{m}$ .

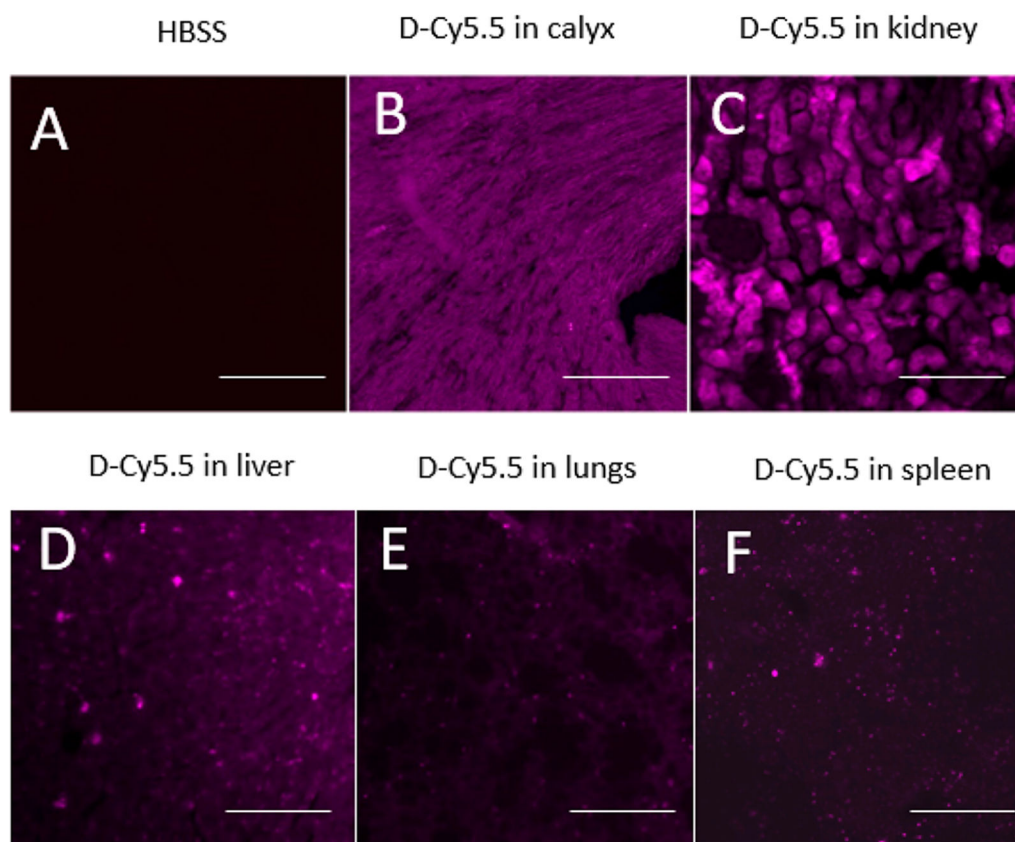


**Figure 5.** Uptake of the D-Cy5.5 by the (B) renal calyx, (C) kidneys, (D) liver, (E) lungs, and (F) spleen following tail-vein injections compared to the (A) control animals. Scale bar = 100  $\mu\text{m}$ .

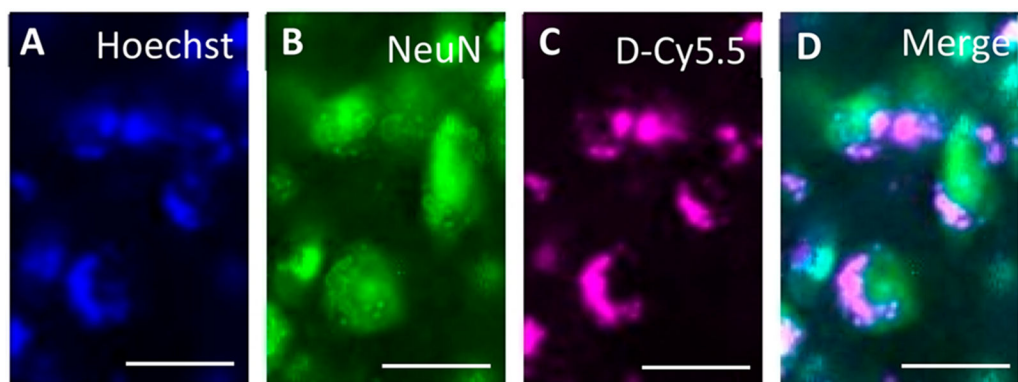


**Figure 6.**

Uptake of D-Cy5.5 by the neurons in the striatum following tail-vein injections. The picture in (A) shows the nuclei of the brain cells stained with Hoechst; (B) shows the neurons stained with NeuN; (C) shows the uptake of D-Cy5.5 by the cells; and (D) shows the merge between Hoechst, NeuN, and D-Cy5.5, confirming that the D-Cy5.5 has been taken up by the neurons in the brain. Scale bar = 20  $\mu\text{m}$ .



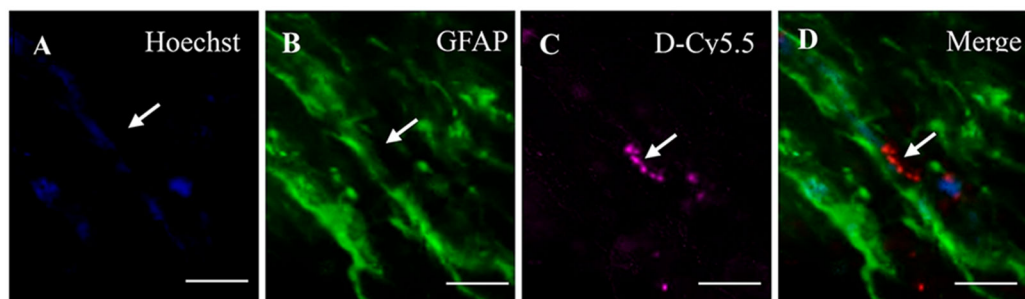


**Figure 7.** Uptake of D-Cy5.5 by glial cells following tail-vein injections. Picture (A) shows the nuclei of the brain cells stained with Hoechst; (B) shows the glial cells stained with GFAP; (C) shows the uptake of D-Cy5.5 by the cells; and (D) shows the merge between Hoechst, GFAP, and D-Cy5.5 confirming that the D-Cy5.5 has been taken by the glial cells in the brain. Scale bar = 20  $\mu\text{m}$ .